Egypt. J. Chem. **Vol. 67**, No. 12 pp. 21 - 36 (2024)

Egyptian Journal of Chemistry

http://ejchem.journals.ekb.eg/

A novel multi-enzyme immobilized biocatalyst for Biodegradation of p,p'- DDT

Tamer Salem [a], Nashwa A.H. Fetyana [a,*], 1 Farag Malhat [b], Ahmed A Abdelhafez [c], Amal I Ramadan [d]

[a] *Soils, Water and Environment Research Institute, Agriculture Research Center, 12619 Giza, Egypt*

[b] *Central Agricultural pesticide laboratory, Agriculture Research Center, 12618, dokki, Giza, Egypt*

[c] *Department of Soils and Water, Faculty of Agriculture, New Valley University- Egypt*
[c] *National Committee of Soil Science, Academy of Scientific Research and Technology- Egypt*
[d] *National Water Research Center (NWRC), Cairo, Egypt*

Abstract

Growing concerns over environmental pollution have necessitated the development of new-generation environmental protection technologies. Multi-enzyme biocatalysts offer a promising approach for reducing pollution caused by organic wastes. However, the recovery of free-form multienzymes is challenging, resulting in high costs and low production efficiency, limiting their application in bioremediation. In this study, we devised a sensitive and stable enzyme biocatalyst by covalently immobilizing multi-enzymes onto nano-silica using glutaraldehyde. Ligninolytic enzymes (laccase, aryl alcohol oxidase, lignin peroxidase, and manganese peroxidase) were produced from Pleurotus ostreatus (NRRL-2366) under submerged fermentation. Enzymes were partially purified through ammonium sulfate precipitation and dialysis. These purified enzymes were immobilized on nano-silica. The resulting immobilized enzymes biocatalyst exhibited stability and activity across a pH range of 4 to 9 and a temperature range of 20 to 55 °C. Immobilization of laccase, lignin peroxidase, manganese peroxidase, and aryl-alcohol oxidase achieved residual activities of 77%, 62.5%, 41.59%, and 28.21%, respectively, after three consecutive batches. Immobilized enzymes biocatalyst effectively degraded p,p'-DDT, and its complete degradation was achieved after incubation at pH 5 and 30 °C for 12 hours, as confirmed by GC-MS analysis . The GC-MS analysis revealed the detection of eleven major metabolites during the degradation process, which were utilized to predict the degradation pathway.

Keywords: Multienzymes; Immobilization; Biocatalyst; p,p'-DDT; Biodegradation, Silica nanoparticles.

1. Introduction

Water is a vital resource that supports all life on Earth. However, concerns about the shortage of freshwater supply and its impact on the sustainability of human societies have been increasing in recent decades [1]. In particular, there has been growing attention to the occurrence and significance of persistent organic pollutants (POPs) in marine environments. POPs are widely distributed, persistent, and toxic compounds that pose various health risks to both humans and the environment. Exposure to these pollutants can result in a wide range of adverse health effects, ranging from acute symptoms such as allergies, hypersensitivity, and dermatological reactions, to more severe consequences like endocrine disruption, reproductive and immune dysfunction, neurological disorders, and cancer. Organochlorine pesticides, including DDT (1,1,1-trichloro-2,2-bis(4-chlorophenyl) ethane), have been extensively used in agriculture and public health since the 1940s [2]. DDT was initially introduced as an organochlorine pesticide during World War II to combat disease-spreading mosquitoes, gaining global popularity as the first synthetic pesticide. Although banned in most countries due to its negative impacts on wildlife and human health[3], DDT is still used for

*Corresponding author e-mail: nashwa.fetyan@arc.sci.eg (Nashwa A. H. Fetyan).
Received date 29 December 2023; revised date 02 October 2024; accepted date 13 June 2024
DOI: 10.21608/ejchem.2024.259255.9113

essential public health and agricultural purposes in some developing nations [4]. Despite the ban, DDT residues remain present in the environment, particularly in flowing water bodies and agricultural soil [5]. Physicochemical processes are commonly employed for DDT removal; however, these methods often involve harsh reaction conditions, generate free radicals and secondary pollutants, and are associated with high operational costs [6]. Therefore, bioremediation processes offer an attractive alternative to these methods. Bioremediation strategies are cost-effective and enable the transformation of DDT and its major byproducts into harmless substances through mineralization [7]. Due to its eco-friendliness and biodegradability, enzymatic degradation of DDT is a favorable approach. However, the free enzyme encounters several limitations, such as poor stability, lack of reusability, and high cost, which hinder its practical application. Immobilization of enzymes, where they are attached to solid supports, can address these limitations by preserving the enzyme's structure and minimizing product contamination [5,8]. Immobilized enzymes offer advantages such as easy recovery, low energy consumption, cost-effectiveness, operational stability, and reusability [5,8].

One such technology is the conversion of agri-food waste into carriers for enzyme immobilization. Crop residues after harvesting, agro-industrial wastes, and fruit and vegetable waste are the most common types of agricultural waste [9], whereas food processing industries generate massive amounts of waste during processing from cereals and pulses, fruits and vegetables, dairy, poultry, meat, egg waste, aquatic life waste, and seafood waste. Furthermore, commercial and residential kitchen garbage complicates waste management [10]

Silica nanoparticles have emerged as promising candidates for immobilization due to their high surface area, pore volume, and lack of UV absorption. Silica and silicon nanomaterials find applications in drug/gene delivery, lightweight aggregates, regenerative medicine, tissue engineering, cancer diagnosis/therapy, catalysis, and energy storage. The demand for eco-friendly synthesis of silica and silicon nanomaterials has increased, focusing on cost-effectiveness, safety, reliability, simplicity, scalability, and controllable particle size distribution. These materials can be obtained from sustainable agricultural resources like rice husk ash, sugar cane, coffee husk, wheat husk, and corn cob ash. The use of green and sustainable techniques eliminates or reduces complex procedures and minimizes environmental contaminants, facilitating the production of advanced materials for high-tech applications [11]. Multi-enzyme biocatalysis is a significant technology used in various industries to produce valuable chemicals. Immobilization of multi-enzymes on support materials has proven to be an efficient approach, enhancing enzymatic activity through substrate channeling and improving enzyme stability and reusability. Various materials, including graphene, carbon nanotubes, metal-organic frameworks, DNA nanostructures, polymers, and silica, have been employed for multi-enzyme immobilization, providing protection against heavy metals, high temperatures, and challenging biological conditions [12,13]. The utilization of nanosilica and multi-enzymes offers a promising solution to overcome the limitations associated with free-form enzymes. Nanosilica provides a stable and efficient support material, while immobilization enhances enzyme stability and activity. This approach addresses the challenges of enzyme recovery, high costs, and low production efficiency, making it a valuable tool for bioremediation and environmental protection [14]

A novel, law coast approach will be done to immobilize different enzymes catalyst on silica nanostructured material for degradation of p,p'-DDT from aqueous solution.

2. Materials and Methods

2.1. Chemicals and media

The standard samples of p,p'-DDT (purity 99.5%), p,p'-DDD (purity 98.0%), p,p'-DDE (purity 98.5%), and DDA (purity 99.0%) were acquired from the Central Agricultural Pesticide Laboratory (CAPL), Agricultural Research Center, Egypt. Analytical-grade sodium sulfate anhydrous, ethyl acetate, n-hexane, and glutraldhyde were obtained from the Aldrich Company.

2.2.1. Fungal strain and culture conditions

The white-rot fungus Pleurotus ostreatus (NRRL-2366) was obtained from the National Central of Agricultural Utilization Research Service, U.S. Department of Agriculture, located in Peoria, Illinois, USA. The fungus was stored at a temperature of 4±1

°C on potato dextrose agar (PDA) slants and sub-cultured every 30 days on fresh medium. Subsequently, it was incubated at 25 ± 1 °C for a period of 7-8 days to facilitate growth.

The cultivation medium for the production of ligninolytic enzymes was prepared following the method described by [15]. Pleurotus ostreatus (NRRL-2366) was grown in a 3-liter medium with the following composition (g/l): glucose (10), (NH4)2SO4 (5.0), yeast extract (5.0), KH2PO4 (2.0), and MgSO4.7H2O (0.3). The medium was supplemented with rice straw (10 g/l) as a carbon source instead of glucose. The cultivation was carried out for 14 days at 28°C and 200 rpm. To inoculate the medium, mycelium from 8-day-old cultures in 400ml Roux flasks, containing 100 ml of medium the same medium . The sterilized medium was inoculated with 5.0 ml of inoculum.

2.2.2. Partial Purification of ligninolytic enzymes

The purification process of ligninolytic enzymes involved several steps. Firstly, extrudates were obtained by squeezing fermented rice straw through muslin cloth and then centrifuged at 8000 rpm and 4 °C for 15 minutes. To obtain crude enzymes, 3 liters of the culture liquid from a 14-day-old culture were concentrated six-fold using ultrafiltration with a 10-kDa cut-off membrane. Polysaccharides were removed from the concentrated solution as described by Guillén et al. [16]. The resulting supernatant was then subjected to ammonium sulfate saturation to precipitate the proteins. After adding an ammonium sulfate solution and incubating at 4 °C for 30 minutes, the precipitates were collected by centrifugation at 10,000g for 10 minutes at 4 °C. The precipitates were subsequently dissolved in 2.5 ml of sodium acetate buffer (25 mM, pH 5.5) , and subjected to dialysis purification using a dialysis membrane with a molecular weight cut-off of 10,000 Dalton at 4 °C in a 25 mM sodium acetate buffer (pH 5.5). The dialysate samples were used to determine protein and ligninolytic enzyme activities [17].

2.2.3. Enzymatic activities and protein content

The enzymatic activities and protein content were measured using culture supernatants at room temperature. The results represent the average of three independent assays. Enzymatic activity was expressed in International units (U), which represents the amount of enzyme needed to produce 1 µmol of product per minute and is expressed as U/L.

Laccase (Lac) activity was determined following the method described by [18]. The substrate used was 2,2'-azinobis-3-ethylbenzthiazoline-6-sulfonate (ABTS), and the oxidation of ABTS was measured by the increase in absorbance at 420 nm. The extinction coefficient used (λ mM = 36 mM-1cm-1). One unit of enzyme activity was defined as the amount of enzyme required to oxidize 1 mmol of ABTS per minute, and the reactions were conducted at 30°C.

Aryl-alcohol oxidase (AAO) activity was determined spectrophotometrically by measuring the oxidation of veratryl alcohol to veratraldehyde. The reaction mixture consisted of 0.1 M sodium phosphate buffer (pH 6.0) and 10 mM veratryl alcohol [19]. Lignin peroxidase (LiP) activity was measured following the method of Tien and Kirk [20], which involved the H2O2-dependent oxidation of veratryl alcohol to veratraldehyde at 25°C and 310 nm. Manganese peroxidase (MnP) activity was measured using 2,6-dimethoxyphenol at 469 nm and 25°C, as described by Kuwahara et al. [21].

For all enzyme activities, 1 U of enzyme activity was defined as the amount of enzyme releasing 1 µmol of oxidized product per minute at 25°C. The total protein content was determined using the Bradford method [22] with bovine serum albumin as the standard.

2.3.1. Synthesis of nano silica powder from rice husk:

The synthesis of nano-silica powder from rice husk was carried out following the methodology described by [23]. Initially, rice husk (RH) was washed with deionized water and dried in an oven at 105 ºC to remove moisture. The dried RH was then calcinated at 700 ºC for 6 hours to obtain silica. Ten grams of the calcinated RH were mixed with 80 mL of a 3.0 M NaOH solution and boiled for 3 hours. The resulting solution was filtered, and the residue was washed with 20 mL of deionized water. The filtrate was allowed to cool to room temperature, and 2.5 M H_2SO_4 acid was added until the pH of the solution reached 2. Subsequently, NH_4OH was added until the pH reached 8.5 at room temperature. The filtrate was dried at 120 ºC for 12 hours, and the resulting sample was powdered. Pure silica was extracted from the sample by refluxing with 6 M HCl for 4 hours, followed by repeated washing with deionized water to remove acidity. The purified silica was separated by centrifugation and dried at 105 ºC

for 2 hours. The pure silica sample obtained from RH was then dissolved in 3.0 M NaOH through continuous stirring for 10 hours. The pH was adjusted to the range of 7.5-8.5 by adding 0.5 M H_2SO_4 drop-wise. The precipitated silica was washed repeatedly with warm deionized water until the filtrate was free from alkali. The precipitate was separated by centrifugation (9000 rpm for 1 hour), and the resulting sample was dried at 50 ºC for 48 hours to obtain nano-silica. Finally, the prepared nano-silica sample was used for immobilizing different catalyst enzymes.

2. 3.2. Immobilization of Oxidoredactase enzymes on nano-silica powder:

In the immobilization process, 0.5g of rice husk silica (RHS) nanocomposite was subjected to multiple washes with 50 mM sodium phosphate buffer (pH 7.2). Subsequently, a solution of 1% glutaraldehyde (GDA) in 50 mM sodium phosphate buffer (pH 7.2) was added to 2.0 g of nano-silica, and the mixture was gently shaken at 25°C for 4 hours to create GDA-linked nano-silica. The proteins were then covalently immobilized onto the GDA-linked nano-silica by incubating them together at 25°C for 24 hours with gentle shaking. Afterward, centrifugation at 3000 rpm was performed to recover the immobilized proteins from the solution. To remove nonspecifically adsorbed proteins, the matrix was washed with 1 M NaCl and 1% Tween 20, followed by 50 mM sodium phosphate buffer (pH 7.2) [24]. The mass of the immobilized proteins was determined by subtracting the mass of the non-immobilized proteins from the total mass. The immobilization efficiency was calculated as the percentage of immobilized protein relative to the total protein.

2.3.3. Characterization of synthesized materials.

The synthesized Nano-SiO2 and Nano-SiO2-Enz materials were characterized using Transmission electron microscopy (TEM) and Fourier transform infrared spectroscopy (FTIR). For TEM analysis, the materials' surface morphology was examined (JEM 2100 HRT high resolution, Japan) after dissolving by ultrasonication and then carried on grid for analysis, with a 10 kV accelerating voltage.

To analyze the functional groups present on the surfaces of Nano-SiO2 and Nano-SiO_2-Enz, Fourier transform infrared spectroscopy (FTIR) was performed. The data were obtained using a Bruker Vertex 80 spectrometer equipped with a Ram-FT module (RAM II). Diffused reflectance style was employed for data generation during FTIR analysis.

2.3.4. Effect of pH and temperature on the activity and stability of the immobilized biocatalyst

The influence of pH on the activities of immobilized enzymes (Lac, AAO, LiP, and MnP) was assessed using spectrophotometric methods. The activities of the immobilized enzymes were measured in various buffer solutions, including 0.05 M Glycine-HCl buffer (pH 1, 2, 3), 0.05 M Sodium acetate buffer (pH 4, 5, 6), and 0.05 M Tris-base buffer (pH 8, 9). To determine the activity of immobilized enzymes, 30 mg of the immobilized enzyme was used [25].

The stability of nano-silica immobilized enzymes at different pH levels was also investigated following a similar method as described by [25]. Both free and immobilized enzymes were incubated at 25 °C in various buffers, including 0.2 M sodium acetate buffers (pH 4.0, 5.0, and 6.0) and 0.2 M phosphate buffer (pH 7.0, 8.0, 9.0, and 10.0), for one hour. The residual activities of the enzymes were then determined. Furthermore, the effect of temperature on enzyme activities was examined in the range of 20–70 °C. Both free enzymes and immobilized enzymes were incubated for 20 minutes at temperatures ranging from 20 to 70 °C in a buffer with pH 7.0. The residual activities were evaluated at 25 °C after cooling. The results for pH and temperature were normalized, with the highest value in each set being assigned 100% activity [26].

2.3.5. Reusability assessment of the immobilized biocatalyst

To assess the reusability of immobilized enzymes obtained using different methods, 0.2 g of the immobilized enzyme was added to an enzyme substrate adjusted to the appropriate pH and incubated at the optimal temperature. Following the initial reaction, the immobilized enzyme was washed with Na-citrate buffer at pH 7.0, and its activity was measured. This process was repeated, and the activity was measured after each subsequent reaction cycle [27]. Throughout all stability experiments, the residual enzymatic activity was determined using the aforementioned method and the initial activity of all enzymes was considered as 100%. This allowed for the comparison of immobilized enzyme activity over

multiple cycles and the assessment of their reusability.

2.4. Biodegradation performance of p,p'- DDT using immobilized of oxidoredactase multi-enzymes

2.4.1. Optimal reaction pH conditions:

To determine the optimal reaction pH conditions, test tubes were prepared with varying pH buffers (5 in total). Each test tube contained 0.5 g of immobilized enzyme and 10.0 mg/L of p,p'-DDT. The test tubes were then incubated in a 30°C water bath for a period of 12 hours. The purpose of this experiment was to evaluate the efficiency of the immobilized oxidoredactase multi-enzymes in degrading p,p'-DDT at different pH levels.

2.4.2. Analysis and measurements

Extraction and determination of metabolites After a 6-hour incubation period, the metabolites of p,p'-DDT were extracted from the supernatant of the cultured cell suspensions that were incubated with p,p'-DDT and p,p'-DDE in a reaction mixture at a concentration of 10 mg/l. To prepare the metabolites for identification, 5 ml of the reaction mixture supernatant was initially extracted with 5 ml of hexane, followed by an additional extraction with 5 ml of ethyl acetate. The organic phase was collected, dehydrated using anhydrous sodium sulfate, and the extracts were combined. After drying with a nitrogen blowing instrument, the volume was adjusted to 5 ml with hexane [28]. The metabolites were analyzed using a Clarus 500 GC/MS system (PerkinElmer, USA) equipped with an autosampler, a splitless model injector, and an Elite-5MS capillary column (crosslinked 5% phenyl-95% methyl silicone, 30 m × 0.25 mm × 0.25 µm). The initial oven temperature was set to 70°C with a hold time of 1.0 minute, followed by an increase to 180°C at a rate of 20°C/min and a hold time of 5.0 minutes. The temperature was then increased by 5°C per minute until reaching 260°C. The injector temperatures were maintained at 250°C. Electron ionization with an electron energy of 70 eV was employed, and the ion source temperature of the mass spectrometer was set to 250°C. The scanning range for the mass spectrometer was from 40 to 550 µ. The transfer line temperature was maintained at 280°C. The metabolites were identified by comparing their retention times and mass spectra with known reference samples. This comparison involved utilizing the mass spectral data provided in the library of WILEY, National Institute of Standard and Technology (NIST-11), as well as the mass spectral data available for p,p'-DDT metabolites in the literature. By examining the retention times and mass spectra, the metabolites were successfully detected and identified.

3. Results and Discussion

3.1. Ligninolytic enzymes production:

Rice straw (1%) was used as a carbon source for fermentation trials. Submerged fermentation of Pleurotus ostreatus NRRL-2366 was conducted at a temperature of 28ºC for duration of 14 days. Figure 1 illustrates the ligninolytic enzyme production ability of the screened strain Pleurotus ostreatus NRRL-2366, including Lac, AAO, LiP, and MnP. The highest activities for Lac, AAO, LiP, and MnP were recorded on the 14th day, with values of 56.60±2.83 U/ml, 13.48±0.55 U/ml, 10.96±0.55 U/ml, and 11.09±0.55 U/ml, respectively. White-rot fungi (WRF) possess a unique extracellular ligninolytic system that oxidizes and breaks down lignin, and P. ostreatus exhibits the ability to produce both hydrolytic and ligninolytic enzymes simultaneously during the fermentation of ligninocellulosic materials [29,30]

The crude enzymes (500 ml) produced after mass production showed a Lac specific activity of 170.481 U/mg, AAO specific activity of 40.548 U/mg , LiP specific activity of 32. 968 U/mg and, MnP specific activity of 33.359 U/mg. Pleurotus ostreatus (NRRL-2366) oxidoredactase enzymes were partially purified from the culture supernatant at 4°C and the purification results are summarized in Table 1. Ammonium sulphate precipitation up to 80% exhibited maximum activity beyond which showed a marked increase in all enzymes specific activates of 255 U/mg, 59.324 U/mg, 46.79 U/mg and 55.102 U/mg for Lac, AAO LiP, and MnP, respectively.

3.2. Characterization of the synthesized nano-silica

TEM images were taken to examine the nanoparticles with and without immobilized catalyst enzyme (Figure 2a, 2b). Diffraction shows that Nano-silica was crystaline and without aggregation, with a grain size ranging from 5nm to 30 nm. In contrast, the TEM images of the nano-SiO_2 catalyst enzyme (Figure 2b) revealed numerous small crystal materials tightly adhered to the surface, with irregular crystal arrangement and micro holes present. This observation suggests that the SiO_2 particles adsorbed

a significant amount of catalyst enzymes, resulting in their irregular appearance.

The FTIR spectrum of the nano silica powder and the nano-silica immobilized with catalyst enzyme is shown in Figure 3(a, b). Figure 3(a) exhibits strong absorption peaks at 447 and 802 cm^{-1}, corresponding to the Si–O–Si bending and Si–H symmetric, respectively. These peaks confirm the presence of highly pure nano silica powder obtained from rice husk. Additionally, a peak at 1062 cm^{-1} is observed, which is assigned to Si-O-Si asymmetric stretching vibration. This further supports the synthesis of the nano-silica formed. In contrast, Figure 3(b) displays additional functional groups at 641, 796 and 3264 cm^{-1}, which are attributed to Aromatic C-H bending (C-H), and Alcohol/Phenol O-H Stretch groups, respectively. These additional functional groups indicate the presence of the immobilized catalyst enzymes.

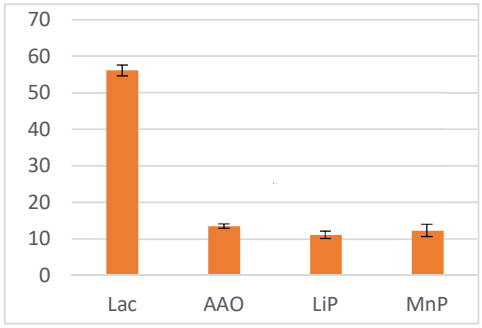

Figure 1: Production of extracellular ligninolytic enzymes, (U/ml), after 14-das growth of Pleurotus ostreatus using rice straw as a carbon source.
- Each value represents the mean ± S.D (Standard Division) and mean of three replicates.
- Values in the same column with the same letter are not significantly at a significance level of $P \leq 0.05$- Lac represents Laccase, AAO represents Aryl-alcohol oxidase, LiP represents Lignin peroxidase, and MnP represents Manganese peroxidase.

The findings suggest that the enzymes laccase (Lac), aryl alcohol oxidase (AAO), lignin peroxidase (LiP), and manganese peroxidase (MnP) derived from Pleurotus ostreatus (NRRL-2366) were successfully immobilized onto nano-silica supports through the utilization of glutaraldehyde as a cost-effective and straightforward method. This immobilization technique, which involves activating the supports with amino groups and employing a glutaraldehyde spacer arm, is commonly used in the biotechnology field to enhance the stability of various enzymes for diverse applications [23,31]. The overall process is depicted in Figure 4.

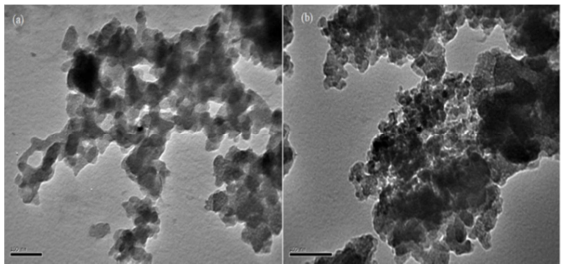

Figure 2: TEM images of Nano-SiO_2 (a), and Nano-SiO_2 immobilized with enzymes (b).

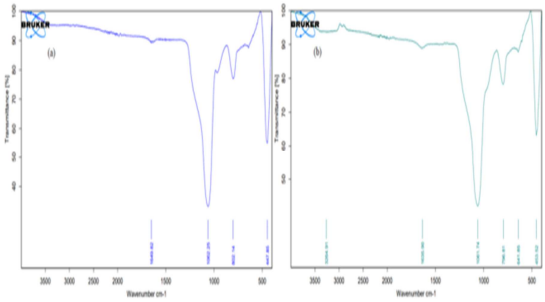

Figure 3: FTIR spectra of nano-SiO_2 (a), and nano-SiO_2 immobilized enzymes (b).

The efficiency of enzyme immobilization was assessed by determining the immobilization-activity yields, which were found to be 86.22±4.55%, 76.11±3.22%, 78.16±1.82%, and 60.21±3.98% for laccase (Lac), aryl alcohol oxidase (AAO), lignin peroxidase (LiP), and manganese peroxidase (MnP), respectively (Figure 5). Covalent binding, using glutaraldehyde as a spacer, offers several advantages in terms of enzyme stability and minimized enzyme leaching. The ordered mesoporous silica provides an ideal platform for covalent immobilization due to its well-defined silanol groups, which offer reactive sites for enzyme functionalization and adjustable surface properties. This enables precise control over the positioning and density of the immobilized catalyst [32–34]. Furthermore, the five-atom carbon chain of glutaraldehyde serves as a spacer for enzymes, facilitating easier accessibility of their active sites to substrates. Glutaraldehyde exhibits rapid reactivity with amine groups, particularly at neutral pH (7), making it more effective than other aldehydes in forming crosslinks that are both thermally and

chemically stable [34] .Vidal-Limon et al. [35] used physical absorption to immobilize Coriollopsis nanostructured silicon foam (MSU-F) in order to create a hybrid nanomaterial (laccase–MSU-F) that would promote the biodegradation of dichlorophen. The nanocomposite exhibited high enzyme gallica laccase on mesoporous synthetic silica foam

adsorption (7 µM/µg MSU-F), indicating that noncovalent interactions (such electrostatic interactions) may play a role in the stabilisation of enzymes within the MSU-F internal pores.

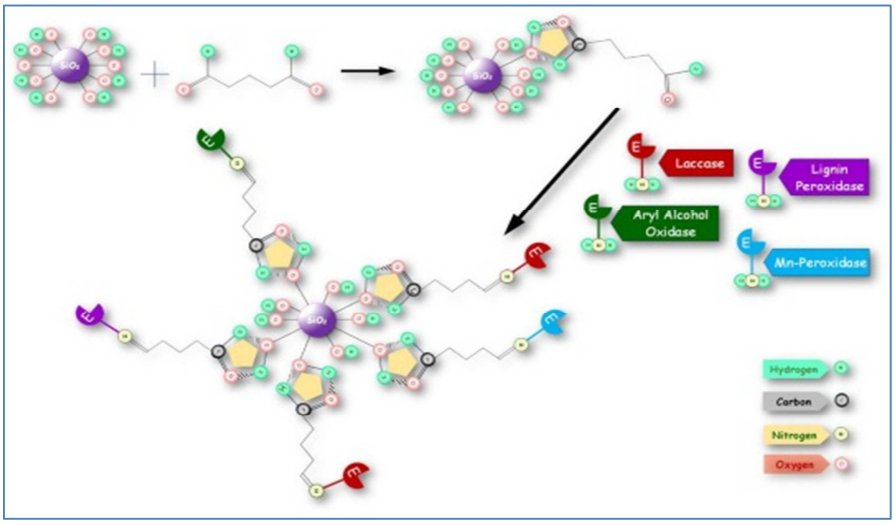

Figure 4: The process of covalent immobilization of multienzymes on nano-silica through activation through glutraldhyde.

Table1: Partial purification of Ligninolytic enzymes from *Pleuratus osteratus*

Ligninolytic enzymes	Purification steps	Total volume (mL)	enzyme activity (U)	Protein (mg)	Specific activity (U/mg)	Purification fold	% Yield
Lac	Crude Extract	500	28300	166.22	170.481	1.0	100
	Ammonium sulphate precipitation	50	1750	6.86	255	1.5	6.18
AAO	Crude Extract	500	6740	166.22	40.548	1.0	100
	Ammonium sulphate precipitation	50	407	6.86	59.324	1.46	6.03
LiP	Crude Extract	500	5480	166.22	32. 968	1.0	100
	Ammonium sulphate precipitation	50	321	6.86	46.79	1.4	5.86
MnP	Crude Extract	500	5545	166.22	33.359	1.0	100
	Ammonium sulphate precipitation	50	378	6.86	55.102	1.7	6.81

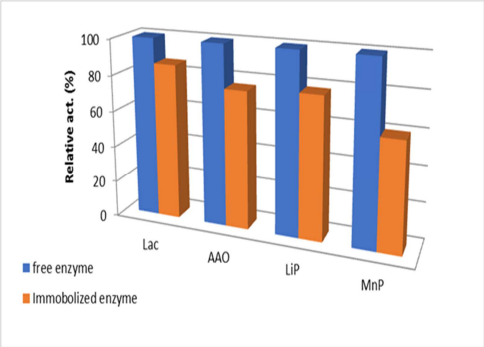

Figure 5: Catalytic activities of immobilized oxidoredactase enzymes (Lac, AAO, LiP, MnP) on nano-silica. The catalytic activity of the free enzyme before immobilization is considered as 100 %.

3.2. Biochemical Characterization of nano-silica immobilized enzymes biocatalyst

The impact of pH on the activities of the immobilized enzymes (Lac, AAO, LiP, and MnP) was examined using spectrophotometric analysis. As depicted in Figure 6a, purified laccase (1 mg/mL) exhibited maximum activity at pH 3.0, whereas the immobilized enzyme (30 mg/mL) showed a shift of one unit towards higher pH values after cross-linking of laccase on nanosilica. This shift can be attributed to the alteration of the microenvironment of laccase by nanosilica, including ionic interactions between the enzyme and charged surfaces of nanosilica. According to Jiang etal, [36], immobilization can create a microenvironment around the enzyme where unequal partitioning of H^+ and OH^- concentrations, resulting from electrostatic interactions with the support, can cause a change in the optimal pH was observed after covalent immobilization of laccase on different supports. For instance, a shift of 0.5 and 1.5 units towards higher pH values was reported when laccase was immobilized on Fe_3O_4-CS-CCn and Fe3O4-CS-EDAC supports, respectively [37]. [38] also demonstrated a shift in the optimum pH for the oxidation of catechol upon immobilization of laccase on magnetic mesoporous nanosilica. In the pH stability test, it was found that the relative activity of the immobilized laccase was retained at approximately 30% at pH 8.0, while the purified laccase was inactive. The silica-laccase nanoparticles exhibited over 90% residual activity within the pH range of 3–5, whereas the purified laccase showed a significant decrease in residual activity within the same pH range (Figure 7a). Similar findings have been reported by several researchers, indicating that the pH stability of laccase improved within the pH range of 2.0–7.0 after immobilization on DEAE-Granocel 500 and sol–gel matrix supports [39-41].

The catalytic rates of immobilized aryl alcohol oxidase (AAO) on nano-silica (30 mg) were compared to those of free AAO (1 mg/mL) at various pH values under the same conditions (Figure 6b). The optimal activity for the immobilized enzyme was observed at pH 6.0-7.0, with relatively high activities retained up to pH 8.0. In contrast, the free enzyme exhibited the highest reaction rate at pH 6.0, and a 50% reduction in activity was observed at pH 8.0. Under acidic conditions (pH 3-4), both free and immobilized AAO enzymes showed similar low activities. These findings suggest that the immobilized AAO enzyme exhibited improved pH stability compared to the free enzyme under alkaline conditions. The pH stability test revealed that almost 35% of the relative activity of immobilized AAO was retained at pH 3, while the purified AAO was inactive. Furthermore, the AAO nanoparticle exhibited over 90% residual activity in the pH range of 6-8, whereas the purified AAO showed a comparable decrease in residual activity within the same pH range (Figure 6b). These results are consistent with the findings of Kato et al.[42] , who reported improved pH stability of AAO immobilized on 3D-mesoporous silicate materials compared to the free enzyme. AAO is primarily active within a neutral to slightly acidic pH range (5.5-7.5), with only a few enzymes active in more alkaline conditions [43]. Immobilization of AAO offers new possibilities for its catalytic activity and stability, opening doors for industrial and biocatalytic applications [44,45]. Figure 6c illustrates the effect of pH conditions on the activity of free (Lignin peroxidase) at 1 mg/mL and immobilized Lip at 30 mg. The results showed that free Lip had maximum activity at pH 3-5, while the highest catalytic activity of nano-silica immobilized Lip ranged between pH 5-7. Moreover, the immobilized Lip exhibited strong acid-base tolerance (Figure 6c). The relative activity of immobilized Lip remained above 90.0% in the pH range of 6-7 and reached 80% and 74% in acidic (pH 4.0) and basic (pH 8.0) solutions, respectively. This enhanced pH stability can be attributed to the protection provided by the carrier and the altered protein structure of the immobilized enzyme, which reduces the influence of pH factors [46]. Free manganese peroxidase (MnP) remained relatively stable in the pH range of 4-6, but rapid inactivation occurred outside of this range (Figure 6d). Previous studies have reported that LiPs from white rot fungi typically exhibit higher activities between pH 2 and

5, and after immobilization, a slight shift towards more acidic conditions is observed [38]. However, LiP from Ganoderma lucidum (GRM117) exhibits optimal pH in basic conditions after immobilization [47]. The purified MnP also remained comparatively stable in the pH range of 4.0-6.0 but was rapidly inactivated outside of this range. The enzyme is susceptible to inactivation at pH 6.5 and higher.

The temperature effects on both free and immobilized enzymes were investigated in the range of 20-70 °C under standard conditions for each enzyme. The optimum temperature for all free and immobilized enzymes was found to be within the range of 25-30 °C (Figures 7a, b, c, and d). After cross-linking laccase on nanosilica, there was an observed shift in the optimum temperature towards higher values. The purified laccase had an optimum temperature of 25 °C, while the immobilized laccase showed optimum activity at 30 °C.

To assess the thermal stability of the enzymes, the residual activity was measured after incubating the free and the immobilized biocatalyst in the absence of substrate at different temperatures (20-70 °C) for 20 minutes (Figures 7a and b). The immobilized biocatalyst demonstrated superior stability, retaining 92%, 83%, 76%, and 63% residual activity after incubation at 55 °C for laccase, AAO, Lip, and MnP, respectively. However, the immobilized biocatalyst became rapidly inactivated at temperatures above this range. In comparison, the free enzymes retained only 80%, 58%, 45%, and 38% residual activity at the same temperature. The enhanced thermo-stability of the immobilized biocatalyst can be attributed to the glutaraldehyde-enzyme cross-linking, which prevents conformational distortion of the enzyme at high temperatures [48,49]. In a simplified view, this strategy achieves multiple intramolecular cross-linking, where the cross-linking agent is a flat and multifunctional structure formed by the activated support surface. This approach enhances enzyme stability against various destabilizing factors, including heat, solvents, and chaotropic reagents [50-52].). Currently, the potential of multipoint covalent immobilization to stabilize enzymes is accepted by the majority of the scientific community [53]. This strategy relies on maintaining the fixed positions of all groups involved in immobilization under any experimental condition, allowing only limited movement determined by the length of the spacer arm. This contributes to improved enzyme stability by reducing conformational changes. Furthermore, it is worth mentioning that cold denaturation, a distinct phenomenon from thermo inactivation, can also induce conformational changes leading to inactive forms of enzymes [54].

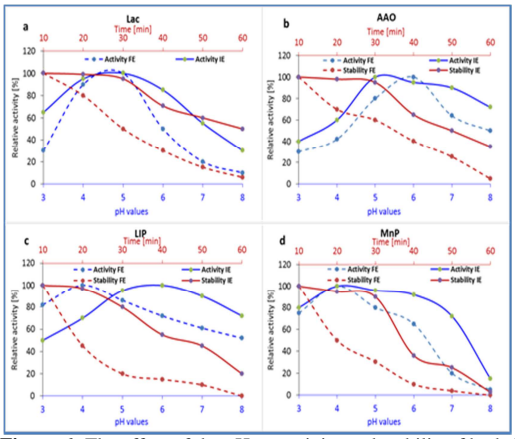

Figure 6: The effect of the pH on activity and stabilityof both free enzyme and immobilized enzymes (IE) (a), laccase (b), Aryl Alcohol Oxidase, (c) Lignin peroxidase, and (d) MnP peroxdase.

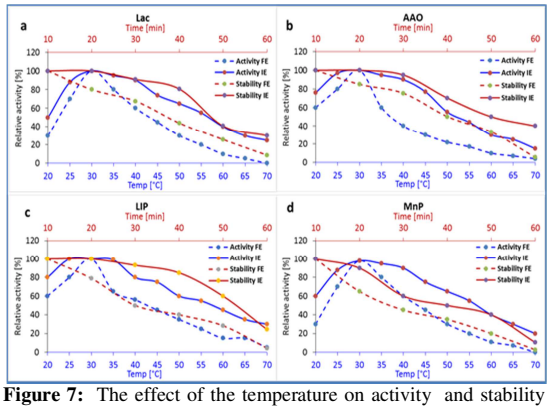

Figure 7: The effect of the temperature on activity and stability of both free enzyme and immobilized enzymes (IE) (a), laccase (b), Aryl Alcohol Oxidase, (c) Lignin peroxidase, and (d) Mn peroxidase.

1.3.3. Reusability assessment of the immobilized enzymes biocatalyst

The reusability of the immobilized biocatalyst was evaluated, as depicted in Figure 8. It was found that the immobilized Lac maintained approximately 77% of its activity after the third cycle, while AAO, Lip, and MnP retained approximately 62.5%, 41.59%, and 28.21% of their activities, respectively. The biocatalyst could be reused for up to five consecutive cycles at a temperature of 30°C. One of the primary objectives of enzyme immobilization is to enable multiple reuse cycles, thereby reducing costs in industrial processes [34]. The ability to reuse the immobilized enzyme for multiple cycles may be attributed to factors such as multipoint, multi-subunit immobilization or the creation of favorable microenvironments [55]. However, a decrease in activity over successive cycles could be attributed to

denaturation, enzyme leakage during use, and diffusional effects [56].

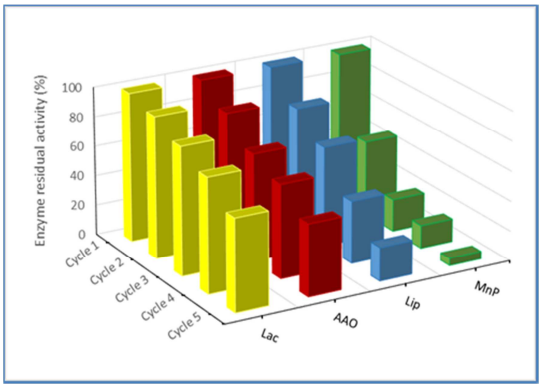

Figure 8: Reusability of the immobilized enzymes biocatalyst

3.4.1. p,p'- DDT degradation efficiency by the immobilized enzymes biocatalyst:

To validate the degradation of p,p'-DDT by the immobilized enzymes biocatalyst and gain insights into potential degradation pathways, the extracted samples were subjected to GC-MS analysis. The results are summarized in Table 2, and the corresponding figures (Figures 9 ,10and 11) provide visual representations of the findings.Data illustrates in Figure 9 and10 revealed that the immobilized multi-enzyme biocatalyst achieved complete degradation of p,p'-DDT (10 mg L^{-1}) under the optimized conditions of pH 5.0, incubated at 30°C for 24 hours. The GC-MS production profile analysis revealed the presence of twelve major metabolites in the experimental samples, including actual and predicted degradation products (Figure11).

These metabolites were compared to the parent p,p'-DDT (1), which had a molecular weight (m/z) of 354 and a retention time (RT) of 19.10 min. The authentic standard of p,p'-DDT listed in the library databases and the control pure compound showed identical characteristics. Notably, the mass-spectral analysis of the samples indicated the presence of a metabolite with a parent ion of m/z 316 and a molecular composition of $C_{14}H_8Cl_4$. This metabolite corresponded to 1,1'-(2,2-dichloroethene-1,1-diyl)bis(4-chlorobenzene) (p,p'-DDE), which is the degradation product of p,p'-DDT and confirmed the involvement of dehydrochlorination of p,p'-DDT to form p,p'-DDE. Further analysis showed the addition of (2H) resulting in the formation of a fragment ion at m/z 318 and a base peak of m/z 246, supporting the molecular composition of $C_{14}H_8Cl_4$ and corresponding to 1,1-trichloro-2,2-bis(4-chlorophenyl)ethane (p,p'-DDD), indicating the transformation of DDT to DDE through dehydrohalogenation and subsequently to DDD via hydrogenation. The degradation pathway also involved the subsequent dechlorination of p,p'-DDD, leading to the formation of 1,1'-(2-chloroethene-1,1-diyl)bis(4-chlorobenzene) (DDMU) with a molecular weight of 283. The formation of DDE, DDD and DDMU indicating the degradation by dechlorination at the trichloromethyl group [2]). Heme-containing enzymes may catalyze reductive dehalogenation, it is also possible that free ferrohemes catalyze reductive dehalogenation in natural environments. Zoro et al. [57]. Immobilized Coriollopsis gallica laccase on mesoporous synthetic silica foam nanostructured silicon foam (MSU-F) efficiently oxidized the dichlorophen pesticide, accompanied by a marked reduced in acute genotoxicity and apoptotic effects [35]. DDMU then underwent hydrogenation to form ethylene], 1,1'-(ethene-1,1-diyl)bis(4-chlorobenzene)(p,p' -DDNU) (metabolite 5) that converted to p,p'-DDOH (metabolite 6), facilitated by the hydroxyl radical oxidation of peroxidases (LiP) [58]. The oxidized compound, bis(4-chloro-3-hydroxyphenyl) acetaldehyde, generated by the action of AAO, exhibited an m/z of 267 and a molecular composition of $C_{14}H_{10}Cl_2O$ (metabolite 7). Further oxidation reactions potentially catalyzed by AAO converted metabolite 6 to bis(4-chlorophenyl) acetic acid (p,p'-DDA) (metabolite 8). The subsequent rings cleavage by laccase through a hydroxyl radical mechanism led to the formation of single-ring aromatic compounds, including 1-(4-chlorophenyl) ethan-1-one (metabolite 9) with m/z 154, 4-chlorobenzaldehyde (metabolite 10) with m/z 140, and 4-methylbenzoic acid (metabolite 11) with m/z 136. The degradation pathway of p,p'-DDT exhibits primarily multidirectional characteristics, as evidenced by the detection of two major hydroxyl derivatives. One of these derivatives, (metabolite 12) with a molecular composition of $C_{14}H_8Cl_4O$ and a mass-to-charge ratio (m/z) of 335, is identified as 2-chloro-5-[2,2-dichloro-1-(4-chlorophenyl) ethenyl] phenol. This hydroxyl derivative undergoes electron and H+ removal from the hydroxyl phenolic group through the action of peroxidases, resulting in the formation

of a phenoxyl radical [59]. Subsequent hydroxyl radical oxidation leads to the generation of a dihydroxylation product with an m/z of 352 and a molecular composition of $C_{14}H_8Cl_4O$, identified as 3,3'-(2,2-dichloroethene-1,1-diyl) bis (6-chlorophenol), referred to as metabolite 13. Notably, peroxidase enzymes play a crucial role in initiating the oxidative dechlorination step during the degradation of various chlorinated phenols [60]. Enzymes produced extracellularly by white-rot fungi exhibit remarkable versatility in their ability to mineralize structurally diverse and highly persistent organic pollutants, which share similarities with lignin. Previous studies have demonstrated variations in the efficiency of enzymatic hydrolysis depending on the specific extracellular products interacting with different substrates [61]. Peroxidases responsible for lignin degradation depend on a source of H2O2, which is supplied through the action of oxidases produced by fungi. Aryl-alcohol oxidases (AAOs, EC 1.1.3.7), also known as veratryl-alcohol oxidases, aromatic alcohol oxidases, or benzyl-alcohol oxidases, are a class of flavin-adenine-dinucleotide (FAD)-containing enzymes that catalyze the oxidation of aromatic and aliphatic allylic primary alcohols, concurrently reducing molecular oxygen to H_2O_2 [62]. The potential of AAOs to efficiently provide hydrogen peroxide for reactions catalyzed by peroxidases and peroxygenases is widely recognized. Additionally, several other flavin-containing oxidases, including vanillyl alcohol oxidase (EC 1.1.3.38) and 4-hydroxymandelate oxidase (decarboxylating; EC 1.1.3.19), possess the ability to oxidize aromatic or phenolic compounds [64-66]. Purnomo et al, [63] reported that under aerobic condition, DDT is metabolized to DDD, DDEand DBP . DDT is metabolized to DDD, dicofol, and 2,2-bis(4-chlorophenyl) acetic acid (DDA) [67, 68]. P. aeruginosa degraded DDT to several metabolic products, such as DDMU, DDMS, DDOH, DDA, 2-hlorobiphenyl, 4-chlorophenyl, 4-chlorobenzoic acid [69]. The glutaraldehyde cross-linking method was used to immobilise laccase on mesoporous silica with a large specific surface area. The degradation process was carried out for 6 hours at 30°C, pH 5.4, and 2,4-Dichlorophenol (with an initial concentration of 50 mg/L) in the presence of 0.1 g of immobilised laccase. The removal ratio and the degradation ratio were 42.28 and 15.93%, respectively. The immobilised laccase has a much higher reusability as compared to free laccase [70].

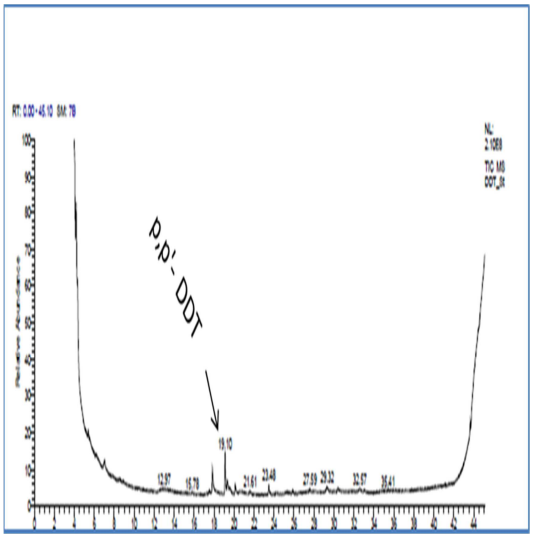

Figure 9: The GC-MS chromatograph of p,p'- DDT before treatment with the immobilized multi enzymes biocatalyst

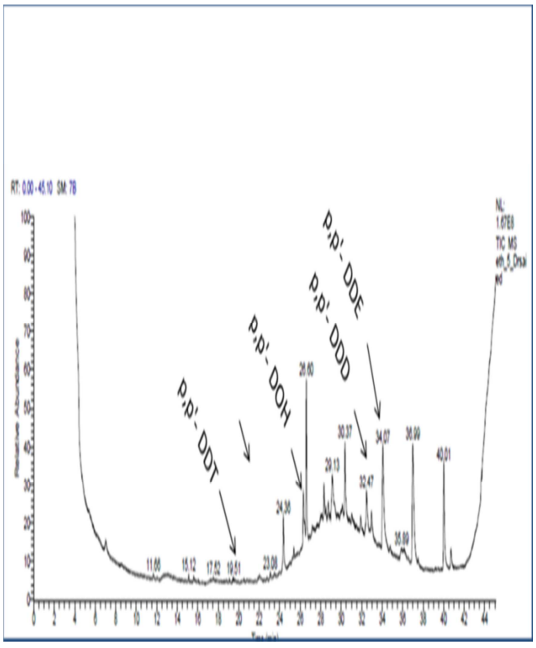

Figure 10: The GC-MS chromatograph of p,p'- DDT and its main metabolites p,p'- DDE, p,p'-DDD, p,p'-DDOH and the other minor metabolites as detected by gas chromatography-mass spectrometry after 12hrs incubation at pH 5 at 30 °.

Table 2: p,p'- DDT and identified p,p'- DDT transformation products detected by GC/MS during biodegradation by the immobilized enzymes biocatalyst

No.	Compound Name	RT (min)	Fragments (*m/z*)	MW	Formula
1	p,p'-DDT	19.10	199, 212, 235,246,354	354	$C_{14}H_9Cl_5$
2	p,p'-DDE	34.06	165, 176, 246, 318	316	$C_{14}H_8Cl_4$
3	p,p'-DDD	32.96	176, 246, 318, 320	318	$C_{14}H_{10}Cl_4$
4	p,p'DDMU	36.07	74,88, 199,213,246	283	$C_{14}H_9Cl_3$
5	p,p'DDNU	ND*	74,88,178,248	249	$C_{14}H_{10}Cl_2$
6	p,p'- DDOH	26.31	199, 213, 255,267	267	$C_{14}H_{10}Cl_2O$
7	bis(4-chloro-3-hydroxyphenyl)acetaldehyde	35.52	125, 246, 265	265	$C_{14}H_{10}Cl_2O$
8	p,p'-DDA	32.96	199,233, 264,281	281	$C_{14}H_{10}Cl_2O_2$
9	4-chlorobenzoic acid	7.04	91,121,136, 139, 154	154	C_8H_7ClO
10	4-chlorobenzaldehyde	7.02	91,121, 136, 140	140	C_7H_5ClO
11	4- methylbenzoic acid	15.76	91, 121, 136	136	$C_8H_8O_2$
12	2-chloro-5-[2,2-dichloro-1-(4-chlorophenyl)ethenyl]phenol	32.96	191, 228, 246, 334	334	$C_{14}H_8Cl_4O$
13	3,3'-(2,2- dichloroethene-1,1-diyl) bis (6-chlorophenol) .	28.74	123,149,222,264,352	350	$C_{14}H_8Cl_4O_2$

ND*; Not Detected (proposed metabolite)

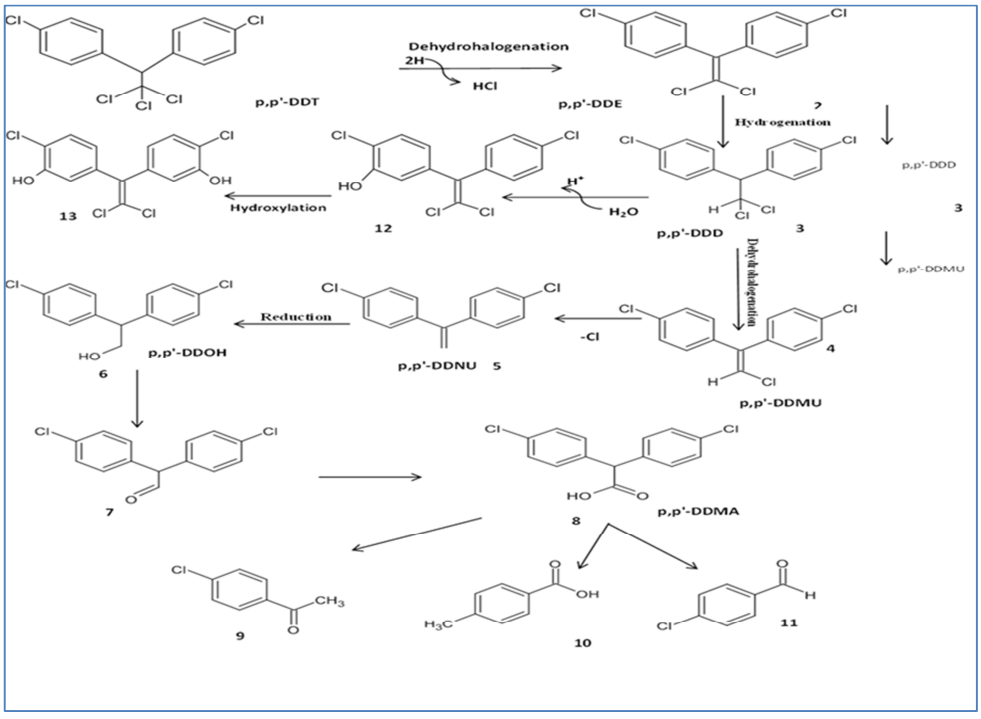

Figure 11: The proposed biodegradation pathway of p,p'- DDT(1) by the immobilized enzymes biocatalyst, (2) p,p'- DDE; (3) p,p'- DDP; (4) p,p'- DDMU ; (5) p,p'- DDOH; (5) bis (4-chloro-3- hydroxyphenyl) acetaldehyde; (6) 1,1'-(ethene-1,1-diyl)bis(4-chlorobenzene ;(7) p,p'- DDMA ; (8) 4-chlorobenzoic acid; (9) 4-chlorobenzaldehyde; (10) 4- methylbenzoic acid, (10) 2-chloro-5-[2,2-dichloro-1-(4-chlorophenyl) ethenyl] phenol ;(11) 3,3'-(2,2- dichloroethene-1,1-diyl) bis (6-chlorophenol) ; (12) 2-chloro-5-[2,2-dichloro-1-(4-chlorophenyl)ethenyl]phenol and (13) 3,3'-(2,2- dichloroethene-1,1-diyl) bis (6-chlorophenol)

Conclusion

We have successfully created a stable and efficient enzyme biocatalyst by immobilizing multi-enzymes onto nano-silica. The immobilized enzymes demonstrated remarkable activity and stability across a wide pH range (4 to 9) and temperature range (20 to 55 °C). This biocatalyst effectively degraded p,p'-DDT, completely eliminating it within a 12-hour incubation period at pH 5 and 30 °C. The analysis also identified eleven major metabolites during the degradation process, indicating the effectiveness of the developed biocatalyst in treating environmental pollution caused by organic wastes. These findings contribute to the advancement of bioremediation technologies and have the potential to significantly impact environmental sustainability. Further investigation into p,p'-DDT degradation by directly ligninolytic enzymes is needed.

Conflict of interest statement

On behalf of all authors, the corresponding author states that there is no conflict of interest.

Data Availability Statement

Data available upon request

References

[1] Rathi B.S. , Kumar P.S. , D.V.N. Vo (2021).criritical review on hazardous pollutants in water environment: Occurrence, monitoring, fate, removal technologies and risk assessment, Sci. Total Environ. 797 : 149134.

[2] Purnomo A.S. , Ashari K. , Hermansyah F. (2017). Evaluation of the Synergistic Effect of Mixed Cultures of White-Rot Fungus Pleurotus ostreatus and Biosurfactant-Producing Bacteria on DDT Biodegradation, J. Microbiol. Biotechnol. 27 :1306–1315.

[3] Auteri D. , Devos Y. , Fabrega J. , Pagani S. , Rortais A. , de Seze G. , Heppner C. , Hugas M.(2022) , Theme (concept) paper – Advancing the Environmental Risk Assessment of Chemicals to Better Protect Insect Pollinators (IPol-ERA) https://doi.org/10.2903/sp.efsa.2022.e200505.

[4] Van den Berg H.(2009). Global status of DDT and its alternatives for use in vector control to prevent disease. Environ Health Perspect. 2009 Nov;117(11):1656-63. doi: 10.1289/ehp.0900785. Epub 2009 May 29. PMID: 20049114; PMCID: PMC2801202.

[5] Zdarta J., Meyer A.S. , Jesionowski T. , Pinelo M.(2018) Developments in support materials for immobilization of oxidoreductases: A comprehensive review, Elsevier B.V, 2018. https://doi.org/10.1016/j.cis.2018.07.004.

[6] Zhang L. , Hu J. , Zhu R. , Zhou Q. , Chen J. (2013). Degradation of paracetamol by pure bacterial cultures and their microbial consortium, Appl. Microbiol. Biotechnol. 97 3687–3698. https://doi.org/10.1007/s00253-012-4170-5.

[7] Ahmed S. , Javed M.A. , Tanvir S. , Hameed A. (2001) Isolation and characterization of a Pseudomonas strain that degrades 4-acetamidophenol and 4-aminophenol, Biodegradation. 12: 303–309. https://doi.org/10.1023/A:1014395227133.

[8] Rathour RK, Bhatia RK, Rana DS, Bhatt AK, Thakur N (2020)F Fabrication of thermostable and reusable nanobiocatalyst for dye decolourization by immobilization of lignin peroxidase on graphene oxide functionalized MnFe2O4 superparamagnetic nanoparticles, Bioresour. Technol. 317 , 124020.

[9] Yaashikaa P. R., Senthil Kumar P., Varjani S. (2022). Valorization of agro-industrial wastes for biorefinery process and circular bioeconomy: A critical review. Bioresour. Technol. 343 126126. 10.1016/J.BIORTECH.2021.126126 [PubMed] [CrossRef] [Google Scholar] [Ref list]

[10] Haldar D., Purkait M. K. (2020). A review on the environment-friendly emerging techniques for pretreatment of lignocellulosic biomass: Mechanistic insight and advancements. Chemosphere 2020:128523. 10.1016/j.chemosphere.2020.128523 [PubMed] [CrossRef] [Google Schol ar]

[11] Habimana P. , Gao J. , Mwizerwa J.P. , Ndayambaje J.B. , Liu H. , Luan P. , Ma L. , Jiang Y. (2021) Improvement of Laccase Activity Via Covalent Immobilization over Mesoporous Silica Coated Magnetic Multiwalled Carbon Nanotubes for the Discoloration of Synthetic Dyes, ACS Omega. 6 2777–2789. https://doi.org/10.1021/acsomega.0c05081.

[12] Alcántara A.R. (2022) Domínguez de María P. , Littlechild J.A. , Schürmann M. , Sheldon R.A. , Wohlgemuth R. , Biocatalysis as Key to Sustainable Industrial Chemistry, ChemSusChem. 15 e202102709. https://doi.org/10.1002/cssc.202102709.

[13] Ren S. , Li C. , Jiao X. , Jia S. , Jiang Y. , Bilal M., Cui J. (2019) Recent progress in multienzymes co-immobilization and multienzyme system applications, Chem. Eng. J. 373 : 1254–1278.

[14] Yang B. , Tang K. , Wei S., Zhai X. , Nie N. (2021) Preparation of Functionalized 29 Mesoporous Silica as a Novel Carrier and Immobilization of Laccase, Appl. Biochem. Biotechnol. 193: 2547–2566. https://doi.org/10.1007/s12010-021-03556-2.

[15] Tellez-Tellez M. , Fernandez F.J. , Montiel-Gonzalez A.M. , Sanchez C. , Diaz- Godinez G. . (2008) Growth and laccase production by Pleurotus ostreatus in submerged and solid-state fermentation, Appl. Microbiol. Biotechnol. 81 , 675e679.

[16] Guillén F. , Martinez A.T. , Martínez M.J. (1990) .Production of hydrogen peroxide by aryl-alcohol oxidase from the ligninolytic fungus Pleurotus eryngii, Appl. Microbiol. Biotechnol. 32 (1990) 465–469. https://doi.org/10.1007/BF00903784.

[17] Ajith S., Ghosh J., Shet D., ShreeVidhya S., Punith B.D., 2019 Elangovan A.V. Partial purification and characterization of phytase from Aspergillus foetidus MTCC 11682. AMB Express. ;9(1):1–11. [PMC free article] [PubMed] [Google Scholar]

[18] Johannes C. , Majcherczyk A. (2000) Laccase activity tests and laccase inhibitors, J. Biotechnol. 78 : 193–199.

[19] Okamoto K., Yanase H. (2002) Aryl alcohol oxidases from the white-rot basidiomycete Pleurotus ostreatus, Mycoscience. 43 : 391–395. https://doi.org/10.1007/s102670200057.

[20] Tien M. , Kirk T. (1984) . Lignin-degrading enzyme from Phanerochaete chrysosporium: purification, characterization, and catalytic properties of a unique H2O2- requiring oxygenase, PNAS 81 :2280e2284.

[21] Kuwahara M. , Glenn J.K. , Morgan M.A. , Gold M.H. . Separation and characterization of two extracellular H2O2-dependent oxidases from ligninolytic cultures of Phanerochaete chrysosporium, FEBS Lett. 169 (1984) 247e250

[22] Bradford, M.M. (1976). A rapid and sensitive method for the quantitation of protein utilising the principle of protein dye binding. Annal. Biochem., 72, 248-254.

[23] Premaratne, W. A. P. J., W. M. G. I. Priyadarshana, S. H. P. Gunawardena, and A. A. P. De Alwis. "Synthesis of nanosilica from paddy husk ash and their surface functionalization." (2013). J. Sci. Univ. Kelaniya 8: 33-48 http://repository.kln.ac.lk/handle/123456789/5451

[24] Le T B, Han C S, Cho K, and Han O. Covalent immobilization of oxylipin biosynthetic enzymes on nanoporous rice husk silica for production of cis(+)-12-oxophytodienoic acid. Artificial Cells, Nanomedicine, and Biotechnology.2018,46,8, ;1523-1529.

[25] Almeida, A. F.; Terrasan, C. R. F.; Terrone, C. C.; Tauk-Tornisielo, S. M. & Carmona, E. C (2018). Biochemical properties of free and immobilized Candida viswanathii lipase on octyl-agarose support: Hydrolysis of triacylglycerol and soy lecithin. Process Biochemistry 65 71–80. http://dx.doi.org/10.1016/j.procbio.2017.10.019

[26] Liu Y, Zeng Z. , Zeng G. et al., 2012 "Immobilization of laccase on magnetic bimodal mesoporous carbon and the application in the removal of phenolic compounds," Bioresource Technology, vol. 115, pp. 21–26,. View at: Publisher Site | Google Scholar

[27] Rahim S.N.A. , Sulaiman , F. Hamzah, K.H.K. Hamid, M.N.M. Rodhi, M. Musa, N.A. Edama, Enzymes encapsulation within calcium alginate-clay beads: Characterization and application for cassava slurry saccharification, Procedia Eng. 68 (2013) 411–417. https://doi.org/10.1016/j.proeng.2013.12.200.

[28] Xie H, Zhu L, Wang J, Jiang J, Wang J. Biodegradation of DDE and DDT by bacterial strain stenotrophomonas sp. DXZ9. J Environ Anal Toxicol. 2017;7: 476-484

[29] Lundell T.K. , Mäkelä M.R. , Hildén K. (2010), Lignin-modifying enzymes in filamentous basidiomycetes - Ecological, functional and phylogenetic review, J. Basic Microbiol. 50 : 5–20. https://doi.org/10.1002/jobm.200900338.

[30] Ergun, S. O.; Urek, R. O. 2017, Production of Ligninolytic Enzymes by Solid-State Fermentation Using Pleurotus ostreatus. Ann. Agrar. Sci. 15, 273–277. DOI: 10.1016/j.aasci.2017.04.003

[31] Yuvakkumar , R., Elango , V., Rajendran, V. and Kannan N. 2014. High-purity nano silica powder from rice husk using a simple chemical method, Journal of experimental Nanoscience, 9:3, 272-281, DOI: 10.1080/17458080.2012.656709

[32] Alptekin Ö. , Seyhan Tükel S. , Yildirim D. , Alagöz D. , Covalent immobilization of catalase onto spacer-arm attached modified florisil: Characterization and application to batch and plug-flow type reactor systems, Enzyme Microb. Technol. 49 (2011) 547–554. https://doi.org/10.1016/j.enzmictec.2011.09.002.

[33] Nimni M.E. , Cheung D. , Strates B. , Kodama M. , Sheikh K. , Chemically modified collagen: A natural biomaterial for tissue replacement, J. Biomed. Mater. Res. 21 (1987) 741–771.

[34] Abdel-Sater M. , Hussein N. , Fetyan N. , Gad S. , Immobilization of Cellulases Produced by Penicillium brevicompactum AUMC 10987, using Cross-Linkage, Chitosan-Coating and Encapsulation, Catrina Int. J. Environ. Sci. 18 (2019) 139–149. https://doi.org/10.21608/cat.2019.28624.

[35] Vidal-Limon, A., Garcia Suarez, P.C., Arellano-Garcia, E., Contreras, O.E., Aguila, S.A., 2018. Enhanced degradation of pesticide dichlorophen by laccase immobilized on nanoporous materials: a cytotoxic and molecular simulation investigation. Bioconjug. Chem. 29 (4), 1073–1080

[36] Jiang D.S. , Long S.Y. , Huang J. , Xiao H.Y. , Zhou J.Y. , Immobilization of Pycnoporus sanguineus laccase on magnetic chitosan microspheres, Biochem. Eng. J. 25 (2005) 15–23.

[37] Kalkan N.A. , Aksoy S. , Aksoy E.A. , Hasirci N. , Preparation of chitosan-coated magnetite nanoparticles and application for immobilization of laccase, J. Appl. Polym. Sci. 123 (2012) 707–7016. https://doi.org/10.1002/app.

[38] wang S. H , Lee K.T. , Park J.W. , Min B.R. , Haam S. , Ahn I.S. , Jung J.K. , Stability analysis of Bacillus stearothermophilus L1 lipase immobilized on surface-modified silica gels, Biochem. Eng. J. 17 (2004) 85–90.

[39] Al-Adhami, A.J., Bryjak, J., Greb-Markiewicz, B., Peczyn´skaCzoch, W.: Immobilization of wood-rotting fungi laccases on modified

cellulose and acrylic carriers. Process Biochem. 37, 1387–1394 (2002)

[40] Irshad, M., Bahadur, B.A., Anwar, Z., Yaqoob, M., Ijaz, A., Iqbal, H.M.N.: Decolorization applicability of sol–gel matriximmobilized laccase produced from Ganoderma leucidum using agro-industrial waste. BioResources 7, 4249–4261 (2012)

[41] Gahlout M. , Rudakiya D.M. , Gupte S. , Gupte A. , Laccase-conjugated amino-functionalized nanosilica for efficient degradation of Reactive Violet 1 dye, Int. Nano Lett. 7 (2017) 195–208. https://doi.org/10.1007/s40089-017-0215-1.

[42] Kato K, Seelan S, Saito T. Catalytic activity of aryl alcohol oxidase immobilized in 3D-mesop- orous silicates. Journal of bioscience and bioengineering. 2009 Oct 1;108(4):310-3.

[43] Goswami, P., Chinnadayyala, S.S.R., Chakraborty, M. et al. An overview on alcohol oxidases and their potential applications. Appl Microbiol Biotechnol 97, 4259–4275 (2013). https://doi.org/10.1007/s00253-013-4842-9

[44] Kim, S., Suzuki, N., Uematsu, Y., and Shoda, M.: Characterization of aryl alcohol oxidase produced by dye-decolorizing fungus, Geotrichum candidum Dec1, J. Biosci. Bioeng., 91, 166–172 (2001).

[45] Buhler, B. and Schmid, A.: Process implementation aspects for biocatalytic hydrocarbon oxyfunctionalization, J. Biotechnol., 113, 183–210 (2004)

[46] Kiani M. , Mojtabavi S. , Jafari-Nodoushan H. , Tabib S.R. , Hassannejad N. , Faramarzi M.A., Fast anisotropic growth of the biomineralized zinc phosphate nanocrystals for a facile and instant construction of laccase@Zn3(PO4)2 hybrid nanoflowers, Int. J. Biol. Macromol. 204 (2022) 520–532.

[47] Oliveira SF, da Luz JM, Kasuya MC, Ladeira LO, Junior AC. Enzymatic extract containing lignin peroxidase immobilized on carbon nanotubes: Potential biocatalyst in dye decolourization. Saudi journal of biological sciences. 2018 May 1;25(4):651-9. https://doi.org/10.1016/j.sjbs.2016.02.018.

[48] D. Panwar, G.S. Kaira, M. Kapoor, Cross-linked enzyme aggregates (CLEAs) and magnetic nanocomposite grafted CLEAs of GH26 endo-β-1,4-mannanase: Improved activity, stability and reusability, Int. J. Biol. Macromol. 105 (2017) 1289–1299.

[49] U. V. Sojitra, S.S. Nadar, V.K. Rathod, A magnetic tri-enzyme nanobiocatalyst for fruit juice clarification, Food Chem. 213 (2016) 296–305.

[50] Inoue M. , Hayashi T. , Hikiri S. , Ikeguchi M. , Kinoshita M. , Mechanism of globule-to-coil transition of poly(N-isopropylacrylamide) in water: Relevance to cold denaturation of a protein, J. Mol. Liq. 292 (2019) 111374.

[51] Parui S. , Jana B. , Cold denaturation induced helix-to-helix transition and its implication to activity of helical antifreeze protein, J. Mol. Liq. 338 (2021). https://doi.org/10.1016/j.molliq.2021.116627.

[53] Weltz J.S., Kienle D.F. , Schwartz D.K. , Kaar J.L. , Reduced Enzyme Dynamics upon Multipoint Covalent Immobilization Leads to Stability-Activity Trade-off, J. Am. Chem. Soc. 142 (2020) 3463–3471.

[54] Yang C. , Jang S. , Pak Y. , Computational Probing of Temperature-Dependent Unfolding of a Small Globular Protein: From Cold to Heat Denaturation, J. Chem. Theory Comput. 17 (2021) 515–524. https://doi.org/10.1021/acs.jctc.0c01046.

[55] Xu J. , Sun J. , Wang Y. , Sheng J. , Wang F. , Sun M. , Application of iron magnetic nanoparticles in protein immobilization, Molecules. 19 (2014) 11465–11486. https://doi.org/10.3390/molecules190811465.

[56] Ye P. , Xu Z.K. , Wu J. , Innocent C. , Seta P. , Nanofibrous poly(acrylonitrile-co-maleic acid) membranes functionalized with gelatin and chitosan for lipase immobilization, Biomaterials. 27 (2006) 4169–4176.

[57] Zoro, J. A., J. M. Hunter, G. Eglinton, and G. C. Ware. 1974. Degradation of p,p'-DDT in reducing environments. Nature (London) 247:235-237.

[58] Maqbool, Z., Hussain, S., Imran, M., Mahmood, F., Shahzad, T., Ahmed, Z., Muzammil, S., 2016. Perspectives of using fungi as bioresource for bioremediation of pesticides in the environment: a critical review. Environ. Sci. Pollut. Res. 23 (17), 16904–16925.

[59] Nadar S.S. , Muley A.B. , Ladole M.R. , Joshi P.U. , Macromolecular cross-linked enzyme aggregates (M-CLEAs) of α-amylase, Int. J. Biol. Macromol. 84 (2016) 69–78.

[60] Mohamed M.S.M. , Asair A.A. , Fetyan N.A.H. , Elnagdy S.M. , Complete Biodegradation of Diclofenac by New Bacterial Strains: Postulated Pathways and Degrading Enzymes, Microorganisms. 11 (2023) 1445. https://doi.org/10.3390/microorganisms11061445

[61] Wang Y. , Shao Y. , Zou X. , Yang M. , Guo L., Synergistic action between extracellular products from white-rot fungus and cellulase significantly improves enzymatic hydrolysis, Bioengineered. 9 (2018) 178–185. https://doi.org/10.1080/21655979.2017.1308991.

[62] Urlacher VB, Koschorreck K. Pecularities and applications of aryl-alcohol oxidases from fungi. Appl Microbiol Biotechnol. 2021 May;105(10):4111-4126. doi: 10.1007/s00253-021-11337-4. Epub 2021 May 17. PMID: 33997930; PMCID: PMC8140971.

[64] de Jong E. , van W.J.H. Berkel B. , van der R.P., Zwan Z. , de J.A.M. Bont B. , Purification and characterization of vanillyl-alcohol oxidase from, Eur. J. Biochem. 657 (1992) 651–657.

[65] Ewing T.A. , Gygli G. , Fraaije M.W. , van Berkel W.J.H., Vanillyl alcohol oxidase, in: Enzym., Academic Press, 2020: pp. 87–116.

[66] Martin C. , Binda C. , Fraaije M.W. , Mattevi A. , The multipurpose family of

flavoprotein oxidases, in: Enzym., Academic Press, 2020: p. 47.
[67] Cùany A, Pralavorio M, Pauron D, Berge JB, Fournier D, Blais C. 1990. Characterization of microsomal oxidative activities in a wild-type and in a DDT resistant strain of Drosophila melanogaster. Pestic. Biochem. Physiol. 37: 293-302.
[68] Joußen N, Heckel DG, Haas M, Schuphan I, Schmidt B. 2008. Metabolism of imidacloprid and DDT by P450 CYP6G1 expressed in cell cultures of Nicotiana tabacum suggests detoxification of these insecticides in Cyp6g1-overexpressing strains of Drosophila melanogaster, leading to resistance. Pest Manag. Sci. 64: 65-73
[69] Bidlan R. 2003. Studies on DDT degradation by bacterial strains. PhD Thesis, Central Food Technological Research Institute, University of Mysore, India. ttp://eprints.csirexplorations.com/id/eprint/169
[70] Yang Y, Xu Y, Yang Y, Yang H, Yuan H, Huang Y, Liu X. Laccase immobilized on mesoporous SiO2 and its use for degradation of chlorophenol pesticides. Russian Journal of Physical Chemistry A. 2016 Sep 18;10(90):2044-54.